Proceedings of the 36th AIAA Thermophysics Conference, AIAA Paper 2003-3493, 2003

Evolution of a Plume in Laser Ablation: Dependence on the Spot Size

Michael I. Zeifman,[a] Barbara J. Garrison,[a] Leonid V. Zhigilei[b]

[a] *Department of Chemistry, The Pennsylvania State University, 152 Davey Laboratory, University Park, PA 16802, USA*

[b] *Department of Material Science and Engineering, University of Virginia, 116 Engineer's Way, Charlottesville, Virginia 22904-4745, USA*

ABSTRACT

The interaction of a powerful laser beam with a target material may result in the formation of a plume, which consists of gas molecules and molecular clusters directly ejected from the surface. A hybrid Molecular Dynamics – direct simulation Monte Carlo scheme capable to model the formation and evolution of the multi-component plume has been proposed recently. In the present study, the first objective is precise characterization of various types of collisions and other reactions among the molecules and clusters with the aid of molecular dynamics simulations. The updated scheme is then applied to study the effect of laser spot size on the evolution of the plume. The increased number of reactions per particle for larger spot size smoothed out a typical two-fold monomer density profile observed for smaller spot sizes.

INTRODUCTION

Several applications of laser ablation, such as thin film deposition and biological mass-spectrometry require detailed modeling of the ablated vapor cloud (plume). The modeling of the plume evolution is challenging because of the diversity of the time- and length-scales of the processes involved in the ablation phenomenon and the complex composition of the ablation plume that may contain a large number of directly ejected molecular clusters of different sizes.[1] Recently, we proposed a two-stage computational model to study the process of the formation and evolution of the plume.[2] In this model, the ablation plume formation is described by the Molecular Dynamics (MD) breathing sphere model[3] and the following long-term plume expansion into a vacuum is modeled by a direct simulation Monte Carlo (DSMC) method. The developed statistical protocol[4] establishes a reliable information transfer between the MD and DSMC parts of the hybrid model. In the present study, the MD trajectories are used to precisely characterize reactions among clusters and molecules, and the updated hybrid model is used to study the dependence of the plume evolution on the simulated laser spot size.

The paper is organized as follows. A brief description of the hybrid two-stage computational method is given in the next section; various types of collisions and other reactions among the plume particles are characterized thereafter and, finally, the results of the large-scale hybrid calculations of evolution of the plumes ejected from small and large laser spots are given and explained.

COMPUTATIONAL METHOD

Complete details of the MD breathing sphere model, used for simulation of the initial stage of the laser ablation process, are given in Ref. 3. The model assumes that each molecule (or appropriate group of atoms) can be represented by a single particle. The parameters of interparticle interaction are chosen to reproduce the properties of an organic material, in this case a molecular solid. In order to simulate molecular excitation by photon absorption and vibrational relaxation of the excited molecules, an additional internal degree of freedom is attributed to each molecule. This internal degree of freedom, or breathing mode, is realized by allowing the particles to change their sizes. The parameters of a potential function ascribed to the internal motion can be used to change the characteristic frequency of the breathing mode and to affect the coupling between internal and translational molecular motions. The laser irradiation is simulated by vibrational excitation of molecules that are randomly chosen during the laser pulse duration within the penetration depth appropriate for a given wavelength. Vibrational excitation is modeled by depositing a quantum of energy equal to the photon energy into the kinetic energy of internal motion of a given molecule.

Since in this model each molecule is represented by a single particle and explicit atomic vibrations are not followed, the system size and the time-step in the numerical integration of the equations of motion can be large enough to reproduce the collective dynamics leading to laser ablation and damage on the time length of up to few nanoseconds.

The MD breathing sphere model is computationally limited in both time (few nanoseconds) and length (a few tens of nanometers). At about one nanosecond after the laser irradiation, the local Knudsen number in the ablated plume becomes high enough to provide the rarified conditions. Therefore, the following long-term plume evolution can be modeled using the DSMC method. In order to adopt the results of an MD simulation as an input for a DSMC calculation, we have to characterize the MD output in terms of statistical distributions (e.g., spatial monomer and cluster distributions, translational and internal energy distributions) and to include an adequate description of all possible reactions among monomers and clusters during the plume expansion into the DSMC model.

The presence of clusters, which comprise a major part of the ejected plume mass, poses the main computational challenge. The extremely low proportion of large-size clusters hinders both statistical description of their parameters based on the results of MD simulations and the following representation of each cluster size as a separate species, as required in the conventional DSMC. Therefore, a new computational scheme, which treats the size of large clusters as a random variable, is developed. The analytical models are proposed and verified for the distributions of translational and internal energy of monomers and clusters and for the distribution of the cluster sizes, required for the information transfer between the MD and DSMC parts of the hybrid model.

Since the minimum number of trace large clusters per cell must be maintained and the number of cells is proportional to the spot size, the proposed method becomes computationally prohibitive for relatively large laser spot sizes. As a remedy, we use a two-system cell structure in which the cell size of the first system is of the order of the mean free path of the well-represented species (molecules and small clusters) and the cell size of the second system is of the order of the mean free path of the trace species (large clusters).

CHARACTERIZATION OF CLUSTER REACTIONS

In order to elucidate the reaction types, their cross sections and distribution of the products in the DSMC calculations, separate molecular dynamics (MD) trajectory studies are performed. As discussed above, the intermolecular interaction in the MD model is described by the Morse potential. In addition, an additional internal potential controls an internal "breathing" degree of freedom associated with each molecule. This representation of a molecule corresponds to the true translational degrees of freedom and one approximate internal degree of freedom, or breathing mode. Our initial studies of this material[2] as well as published studies of other materials[5] suggest that the following interactions are typical in the rarified regime.

a. Simple collisions
$$A_i + A_j \rightarrow A_{i+j}^* \rightarrow A_i + A_j$$

b. Stripping/rearrangement collision ($i+j=k+l$)
$$A_i + A_j \rightarrow A_{i+j}^* \rightarrow A_k + A_l$$

c. Fragmentation collision ($i+j=k+l+m+\ldots$)
$$A_i + A_j \rightarrow A_{i+j}^* \rightarrow A_k + A_l + A_m + \ldots$$

d. Sticking collision
$$A_i + A_j \rightarrow A_{i+j}^*$$

e. Thermal decomposition or evaporation of a small (monomer, dimer, etc.) cluster
$$A_i \rightarrow A_{i-j} + A_j$$

Here, A_i stands for a cluster of i monomers, i=1,2,..., and A_{i+j}^* stands for a collision complex of clusters of sizes i and j.

To implement the above reactions in the DSMC method, their probabilities must be estimated. Then, the reaction rates must be characterized in terms of cross sections, post-reaction velocities in terms of velocity and scattering-angle distributions, and internal energy in terms of rotational and vibrational energy distributions. In principle, the reaction probabilities, cross sections, and the distributions can be estimated by separate MD trajectory studies. However, taking into account the wide spectrum of the input parameters, such as relative velocity, cluster structure, rotational and vibrational energies (see Fig. 1), direct estimation of these quantities quickly becomes formidable for the cluster size range observed in MD simulations of laser ablation (up to several thousand of molecules). The proposed remedy is to use available theoretical models and estimate their parameters using just a few trajectories. Below we explain in detail each reaction type.

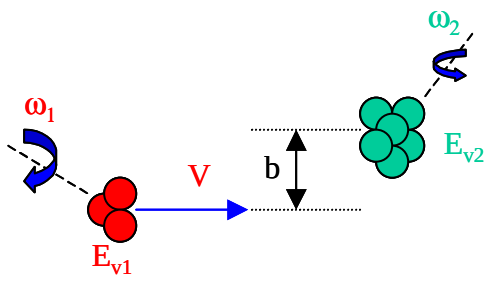

Figure 1. Schematic representation of a binary collision. Each particle is characterized by its orientation, angular velocity (ω) and vibrational energy (E_v). The impact parameter is given by b.

Simple Collisions. For monomer-monomer collisions we calculate the cross sections based on the maximum value of the impact parameter at which a nonzero energy transfer occurs.[6] The dependence of the calculated cross sections (σ) on relative velocity (c) follows the variable hard sphere (VHS) and variable soft sphere (VSS) models[7]

$$\frac{\sigma}{\sigma_{ref}} = \left(\frac{c_{ref}}{c} \right)^{\nu}, \qquad (1)$$

where the exponent ν is estimated to be 0.24, and the subscript designates a reference value. The post-collisional distributions of internal and kinetic energies and the distribution of scattering angles significantly deviate from those predicted by available phenomenological models.[8] Since the distribution of scattering angles is of minor importance for DSMC,[9] we approximate it by the cosine distribution in the spirit of the VHS model. To characterize the collisional energy redistribution, we have developed a new phenomenological model in which the post-collisional distributions are skewed with regard to the pre-collision values of the kinetic and internal energies. The details of this model will be reported elsewhere.

Unlike monomer-monomer collisions, the collisions involving larger particles, i.e. monomer-cluster and cluster-cluster collisions, depend on the initial cluster orientation and are not characterized by a step-wise dependence of the collision probability (P) on the impact parameter (b). Therefore, the maximum impact parameter at which the energy transfer still occurs can no longer be used for the cross-section estimation. An alternative approach is to calculate the equivalent cross section by equating the areas below the actual curve P vs. b^2 and that of ideally spherical particles, as shown in Fig. 2. The calculated results are shown in Fig. 3 for clusters up to 30 molecules in size. As can be seen in Fig. 3, the following hard-sphere approximation may be used for the radius (R) of the equivalent cross section:

$$R = 3.97 \cdot \left(N_1^{1/3} + N_2^{1/3} \right) + 3.18, \text{ Å}, \qquad (2)$$

where N_1 and N_2 are the numbers of molecules in the colliding clusters. The dependence of the calculated cross sections on the relative velocity follows Eq. (1), and it can be shown that the exponent ν quickly decreases with the cluster size. The post-collisional distributions of the energies and scattering angles are characterized similarly to the monomer-monomer distributions.

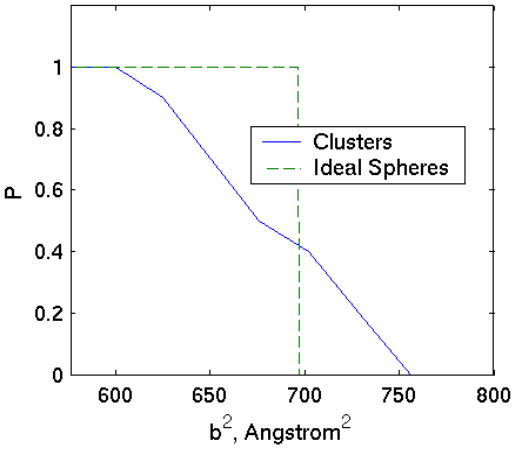

Figure 2. Actual curve P vs. b^2 for collisions between identical clusters of 21 molecules in size and the equivalent curve of ideally spherical particles. Relative velocity is 110 m/s.

Thermal Decomposition. The process of evaporation from internally hot clusters must be characterized in terms of the evaporation rate and the product distributions. A popular model for the evaporation rate is the RRK model[10] predicting that the rate $\gamma_{N,k}$ of thermal decomposition of a cluster of N molecules with internal energy E_N into clusters of N-k and k molecules is given by

$$\gamma_{N,k} = C_1 \left(\frac{E_N - D_k(N)}{E_N} \right)^{C_2}, \qquad (3)$$

where $D_k(N)$ is the corresponding dissociation energy, and C_1 and C_2 are constants. The constant C_1 is proportional to the number of surface molecules in the cluster of N molecules and to the frequency of molecular vibrations that may lead to the evaporation event. The constant C_2 in the RRK model is the number of available degrees of freedom. To test the RRK model, several MD trajectories were run to study the process of evaporation from internally hot clusters.

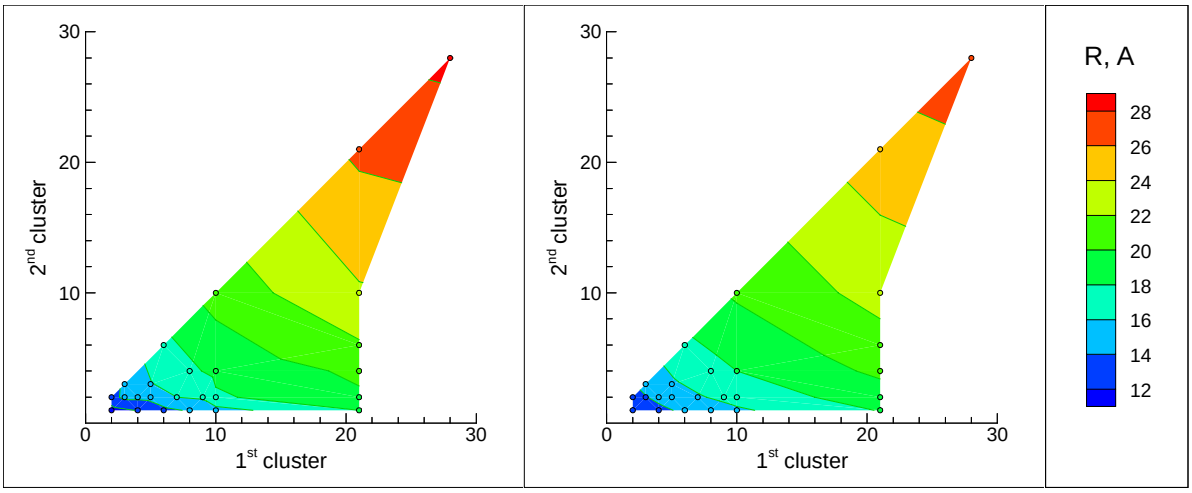

Figure 3. Calculated (left) and approximated by Eq. 2 (right) radus of cross-sections in collisions between clusters of various sizes. The relative velocities correspond to the most probable values at temperatures 600 K and 300 K.

Since the dissociation energy quickly increases with k, monomer evaporation is the most likely channel of cluster decomposition. The results show that for the actual range of cluster temperatures in the ablation plume, monomer evaporations constitute more than 95% of all evaporation events. The estimated constants C_1 and C_2 along with their predictions based on the approximated number of surface molecules and on the number of vibrational degrees of freedom correspondingly are depicted in Figs. 4a and 4b. It can be seen in Fig. 4 that for clusters larger than septamers, the actual and approximated data are in an acceptable agreement.

In addition, the kinetic energy release pertinent to the thermal decomposition reactions was determined. The results of our MD simulations suggest that the distribution function of the energy release (E_r) shared between the monomer and the daughter cluster is adequately represented by the Engelking theory[10]

$$P(E;E_r) = (\xi-2)(\xi-3)E_r \frac{(E-E_r-D_1)^{\xi-4}}{(E-D_1)^{\xi-2}} \qquad (4)$$

where E, ξ and D_1 are the internal energy, the number of degrees of freedom and the monomer evaporation energy of the mother cluster, respectively. The subsequent sharing of this energy between the evaporated monomer and the daughter cluster can be modeled by an inelastic collision as described above.

Sticking Collisions. If the collision complex does not disintegrate during the time of thermalization, the collision is designated as sticking collision. The thermalization time of a collision complex can be approximated by a few periods of molecular vibrations, i.e., a few picoseconds. Numerous studies reported for atomic clusters suggest that the lifetime of the sticking collision complex can be approximated by the RRK model.[5,11] To check if the sticking complex of our molecular clusters can be characterized by this model, several MD simulations have been performed. The results show[8] that no significant difference exists between a hot cluster and a sticking complex of the same size and energy.

Stripping and Fragmentation Collisions. Since a sticking collision followed by an evaporation event can be confused with a stripping collision, we define a stripping/fragmentation collision as a collision whose

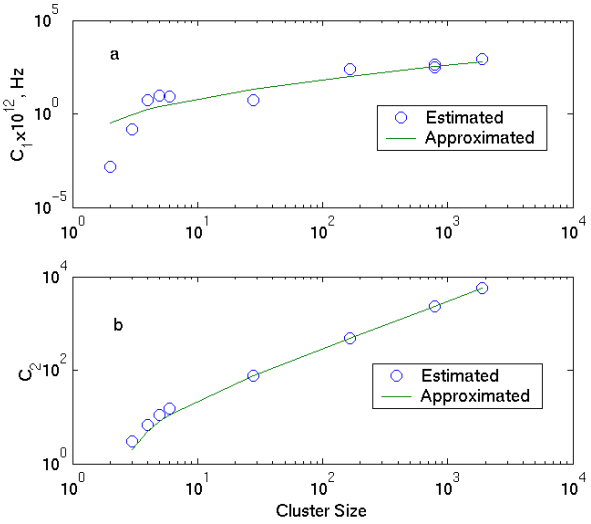

Figure 4. Estimated parameters of the RRK model and their predictions based on the approximated number of surface molecules (a) and on the number of vibrational degrees of freedom (b). The internal temperatures range from 700 K to 400 K.

collision complex disintegrates in a few picoseconds. In this case, the collision complex does not succeed to thermalize and the RRK model cannot be applied. A possible way for characterization of a stripping or fragmentation collision is to model it by an inelastic collision followed by thermal decomposition. The MD studies[8] support this hypothesis.

Reaction Probabilities. The estimated probabilities of the reaction types for several sizes of the colliding clusters are given in Table 1. It is seen from the Table that the sticking collisions dominate for large colliding clusters. The sticking probability P_S can be reasonably approximated by the following empirical formula:

$$P_S = 1 - \exp\{-[0.42 \cdot (N_1^{1/3} + N_2^{1/3})]^4\} \quad (5)$$

Note that unlike the empirical formulae proposed previously,[12] our Eq. (5) yields sticking probability of unity for the infinitely large cluster size.

Cluster sizes	2, 1	3, 1	4, 1	5, 1	6, 1	9, 1	21,1	2,2	2,3	2,4	2,6	3,3	10,10
Sticking probability	0.5	0.6	0.8	0.85	0.86	0.9	0.96	0.5	0.7	0.95	1.0	0.94	1.00
Eq. (5)	0.56	0.67	0.75	0.81	0.86	0.94	0.99	0.71	0.81	0.87	0.94	0.88	1.00

Table 1. Probability of a sticking collision vs. cluster size. The relative velocities correspond to the most probable values at temperature 600 K.

THE EFFECT OF THE LASER SPOT SIZE ON THE PLUME EVOLUTION

The hybrid model updated with the reaction parameterization obtained from MD calculations and the two-system cell structure described earlier is used to study the effect of laser spot size on the plume evolution. Experimental measurements of the velocities and angular distributions are typically performed for monomers only, as the detection of clusters is more difficult and the probability of finding large clusters rapidly decreases as a function of size. Simulations of laser ablation of an organic solid (pulse duration of 15 ps, fluence above the ablation threshold) performed by the hybrid model clearly demonstrate a significant difference between the monomer distributions in the expanding plume for laser spot diameters of 20 μm and 200 μm, Fig. 5. The monomer cloud ejected from the 200 μm spot is characterized by a larger area of high density and a bottle shape, while the monomers ejected from the 20 μm spot form a characteristic two-fold shape, which consists of a slow less forward-peaked fraction and a fast fraction, which is directed more towards the surface normal. These differences can be attributed to the evaporation and condensation reactions between monomers and large clusters. The radial expansion of large clusters occurs mainly due to the collisions between the clusters and monomers. Since the time of plume rarefaction due to the axial expansion is approximately independent of the spot size, large clusters acquire approximately the same terminal radial velocity. Therefore, the relative radial expansion of large clusters is significantly smaller for the larger spot size, as seen in Fig. 6. Accordingly, the concentration of the monomers evaporated from the large clusters is much higher in the case of the larger spot size, leading to a higher monomer density near the plume axis, as seen in Fig. 5. The time-dependence of the rates of condensation and evaporation reactions can explain possible bifurcation of the monomer density profile, Fig.5. For the 20 μm spot, the clusters in the size range of 300 to 1000 molecules expand significantly in the radial direction, quickly cool down, and the evaporations cease early. Since the probability of a monomer-cluster collision is maximal for clusters in this size range, most of the monomers that spatially overlap with these clusters will stick. For the 200 μm spot, the relative radial cluster expansion is small, clusters cool down more slowly and the evaporation ceases much later. In this case, the evaporation will compensate the sticking collisions and no pronounced bifurcation occurs.

Optimization of the proposed computational scheme and realistic representation of experimental conditions are the main directions for further investigation.

ACKNOWLEDGEMENTS

This work was supported through the Free Electron Laser Program by the Air Force Office of Scientific Research.

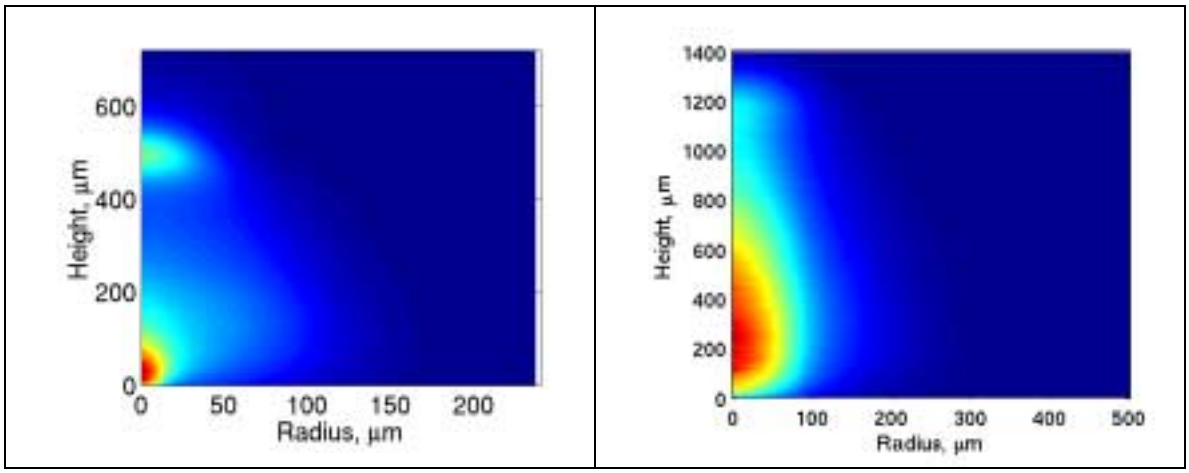

Figure 5. Monomer density at the time when the reactions in the plume cease. Left frame: spot diameter 20 μm, time 300 ns after laser irradiation. Right frame: spot diameter 200 μm, time 760 ns. The aspect ratio is the same in both frames.

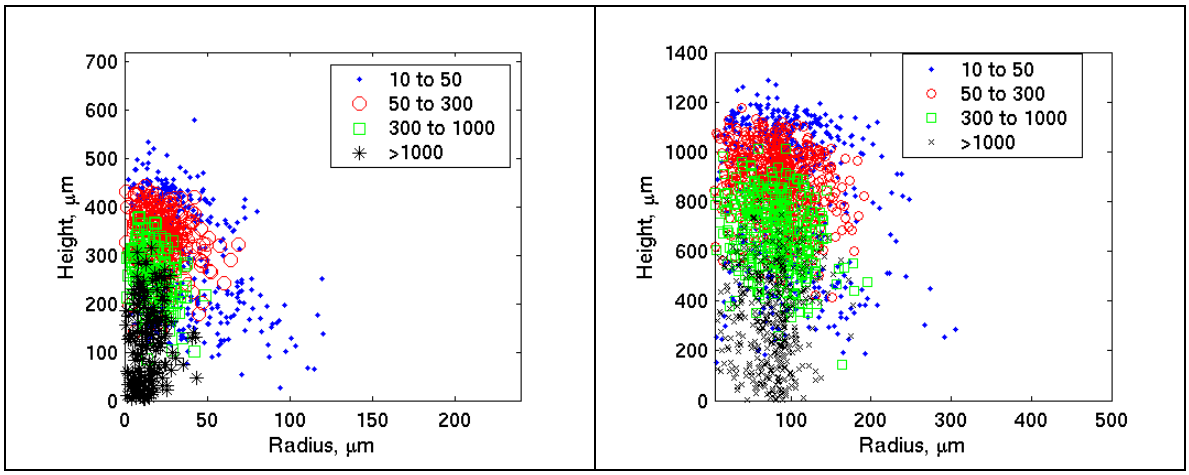

Figure 6. Spatial location of clusters of different sizes in the plume at the time when the reactions in the plume cease. Left frame: spot diameter 20 μm, time 300 ns after laser irradiation. Right frame: spot diameter 200 μm, time 760 ns. Each symbol designates ten clusters (left) or five clusters (right).

REFERENCES

1 L. V. Zhigilei, Appl. Phys. A **76**, 339, 2003.

2 M. I. Zeifman, B. J. Garrison, L. V. Zhigilei, J. Appl. Phys. **92**, 2181, 2002.

3 L. V. Zhigilei, P.B.S. Kodali, B.J. Garrison, J. Phys. Chem. B **101**, 2028 (1997); ibid., **102**, 2845 (1998).

4 M. I. Zeifman, B. J. Garrison, L. V. Zhigilei, Mat. Res. Soc. Symp. Proc. **731**, W3.8.1, 2002.

5 R. Venkatesh et al., J. Chem. Phys. **102**, 7683 (1995); ibid., **104**, 9016 (1996); P. Schaaf et al., J. Chem. Phys. **114**, 8091 (2001); L. Ming et al., J. Phys. Chem. A **101**, 4011 (1997).

6 Y. Sakiyama, S. Takagi, Y. Matsumoto, AIP Conf. Proc. **663**, 304 (2003).

7 G. A. Bird, Molecular Gas Dynamics and the Direct Simulation of Gas Flows (Clarendon Press, Oxford, 1994)

8 M. I. Zeifman, B. J. Garrison, and L. V. Zhigilei, unpublished results.

9 G. A. Bird, private communication.

10 M. F. Jarrold, in Clusters of Atoms and Molecules, edited by H. Haberland (Springer, Berlin, 1994), p. 163.

11 J. W. Brady, J. D. Doll, and D. L. Thompson, J. Chem. Phys. **71**, 2467 (1979); ibid., **73**, 2767 (1980); ibid., **74**, 1026 (1981).

12 H. Hettema and J. S. McFeaters, J. Chem. Phys. **105**, 2816 (1996).